

Newtonian pulsations of relativistic ONe-core ultra-massive DA white dwarfs

A. H. Córscico,¹ L. G. Althaus,¹ and M. Camisassa,²

¹Facultad de Ciencias Astronómicas y Geofísicas, Universidad Nacional de La Plata, Paseo del Bosque s/n, (1900) La Plata, Argentina; acorsico,althaus@fcaglp.unlp.edu.ar

²Departament de Física, Universitat Politècnica de Catalunya, c/Esteve Terrades 5, E-08860 Castelldefels, Spain

Abstract

Ultra-massive H-rich (DA spectral type) white dwarf stars ($M_* > 1.05M_\odot$) are expected to be substantially crystallized by the time they reach the ZZ Ceti instability strip ($T_{\text{eff}} \sim 12\,000$ K). Crystallization leads to a separation of ^{16}O and ^{20}Ne (or ^{12}C and ^{16}O) in the core of ultra-massive WDs, which strongly impacts their pulsational properties. An additional factor to take into account when modeling the evolution and pulsations of WDs in this range of masses are the relativistic effects, which induce changes in the cooling times and the stellar masses derived from the effective temperature and surface gravity. Given the arrival of large amounts of photometric data from space missions such as *Kepler/K2* and *TESS*, it is important to assess the impact of General Relativity in the context of pulsations of ultra-massive ZZ Ceti stars. In this work, we present results of Newtonian gravity(g)-mode pulsation calculations in evolutionary ultra-massive WD models computed in the frame of the General Relativity theory.

1 Introduction

ZZ Ceti stars are pulsating DA (H-rich atmospheres) white dwarfs (WDs) with effective temperatures in the range $10\,500 < T_{\text{eff}} < 12\,600$ K. These variable stars exhibit pulsation periods from ~ 100 s to ~ 1400 s due to nonradial gravity(g) modes with harmonic degree $\ell = 1$ and $\ell = 2$ (Winget & Kepler, 2008; Fontaine & Brassard, 2008; Althaus et al., 2010; Córscico et al., 2019). Although the vast majority of ZZ Ceti stars are DA WDs with masses between ~ 0.5 and $\sim 0.8M_\odot$, g -mode pulsations have also been detected at least in four ultra-massive ($M_* > 1.05M_\odot$) ZZ Ceti stars so far; they are BPM 37093 ($M_* = 1.1M_\odot$ Kanaan et al., 1992), GD 518 ($M_* = 1.24M_\odot$ Hermes et al., 2013),

SDSS J084021 ($M_* = 1.16M_\odot$ Curd et al., 2017), and WD J212402 ($M_* = 1.16M_\odot$ Rowan et al., 2019). It is likely that pulsating WDs even more massive ($M_* > 1.30M_\odot$) will be identified in the coming years with the advent of huge volumes of high-quality photometric data collected by space missions such as the ongoing *TESS* mission (Ricker et al., 2014) and the future *PLATO* space telescope (Rauer et al., 2014). This big amount of data is expected to make asteroseismology a promising tool to study the structure and chemical composition of ultra-massive WDs (Córscico et al., 2019). The increasing number of ultra-massive WDs with masses beyond $1.30M_\odot$, as well as the immediate prospect of detecting pulsating WDs with such masses, demand new appropriate theoretical evolutionary models to analyze them. In particular, it is necessary to calculate models that take into account relativistic effects and to evaluate the impact of General Relativity on the pulsational properties of ultra-massive WDs. In this exploratory investigation, we take the first step in this direction, calculating Newtonian pulsations on fully relativistic equilibrium models.

2 Relativistic WD models

We have generated ultra-massive WD model sequences with ONe cores taking into account the full effects General Relativity employing the LPCODE stellar evolution code (Althaus et al., 2022). We considered realistic initial chemical profiles as predicted by the progenitor evolutionary history (Siess, 2007, 2010; Camisassa et al., 2019), and computed model sequences of $1.29, 1.31, 1.33, 1.35$, and $1.369M_\odot$ WDs. The standard equations of stellar structure and evolution have been generalized to include the effects of General Relativity, following Thorne (1977). For comparison purposes, the same sequences have been computed but for the Newtonian gravity case. We have included the energy released during the crystallization

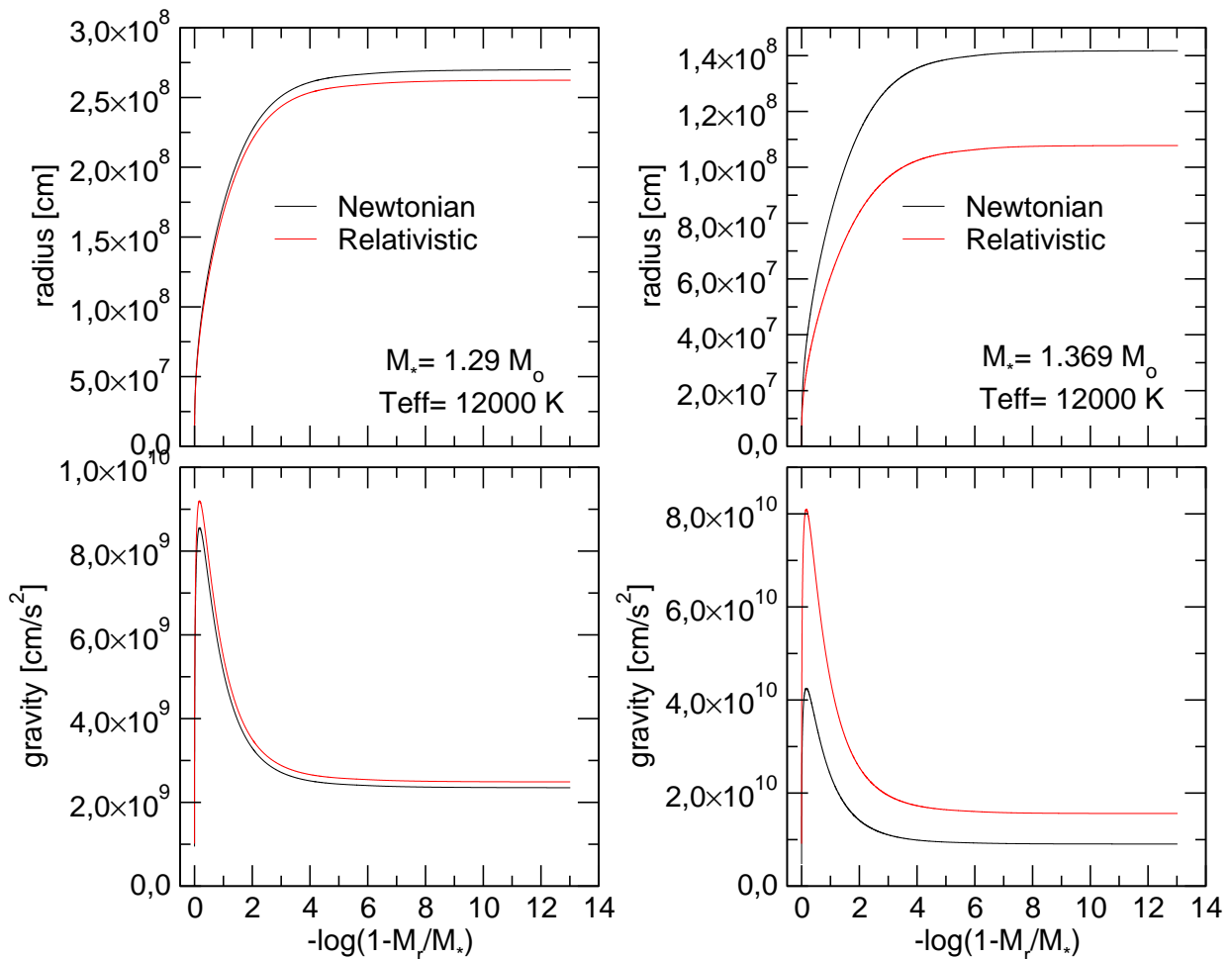


Figure 1: The stellar radius (upper panels) and gravity (bottom panels) in terms of the outer mass fraction coordinate corresponding to ultra-massive DA WD models with $M_* = 1.29 M_\odot$ (left) and $M_* = 1.369 M_\odot$ (right), for the Newtonian case (black curves) and the fully relativistic case (red curves), for $T_{\text{eff}} \sim 12000 \text{ K}$.

process, both due to latent heat and due to the induced chemical redistribution as in Camisassa et al. (2019).

We show in Fig. 1 the stellar radius and gravity of ultra-massive DA WD models with $1.29 M_\odot$ (left panels) and $1.369 M_\odot$ (right panels), for the Newtonian case (black curves) and the fully relativistic case (red curves). Clearly, general relativity induces smaller radii and larger gravities, and this effect is more pronounced for larger stellar masses.

3 Chemical profiles and the Brunt-Väisälä and Lamb frequencies

The cores of our models are composed mostly of ^{16}O and ^{20}Ne and smaller amounts of ^{12}C , ^{23}Na , and ^{24}Mg . Since element diffusion and gravitational settling operate throughout the WD evolution, our models develop pure ^1H envelopes. The ^4He content of our WD

sequences is given by the evolutionary history of progenitor star, but instead, the ^1H content of our canonical envelopes [$\log(M_{\text{H}}/M_*) = -6$] has been set by imposing that the further evolution does not lead to ^1H thermonuclear flashes on the WD cooling track. The temporal changes of the chemical abundances due to element diffusion are assessed by using a new full-implicit treatment for time-dependent element diffusion (Althaus et al., 2020).

The chemical profiles in terms of the fractional mass for $1.29 M_\odot$ and $1.369 M_\odot$ ONe-core WD models at $T_{\text{eff}} \sim 12000 \text{ K}$ and H envelope thickness $\log(M_{\text{H}}/M_*) = -6$ are shown in the upper panels of Fig. 2. At this effective temperature, typical of the ZZ Ceti instability strip, the chemical rehomogenization due to crystallization has already finished, giving rise to a core where the abundance of ^{16}O increases and ^{20}Ne decreases outward.

In the lower panels of Fig. 2 we show the squared Brunt-Väisälä and Lamb ($\ell = 1$) frequencies corresponding to the same models shown in the upper pan-

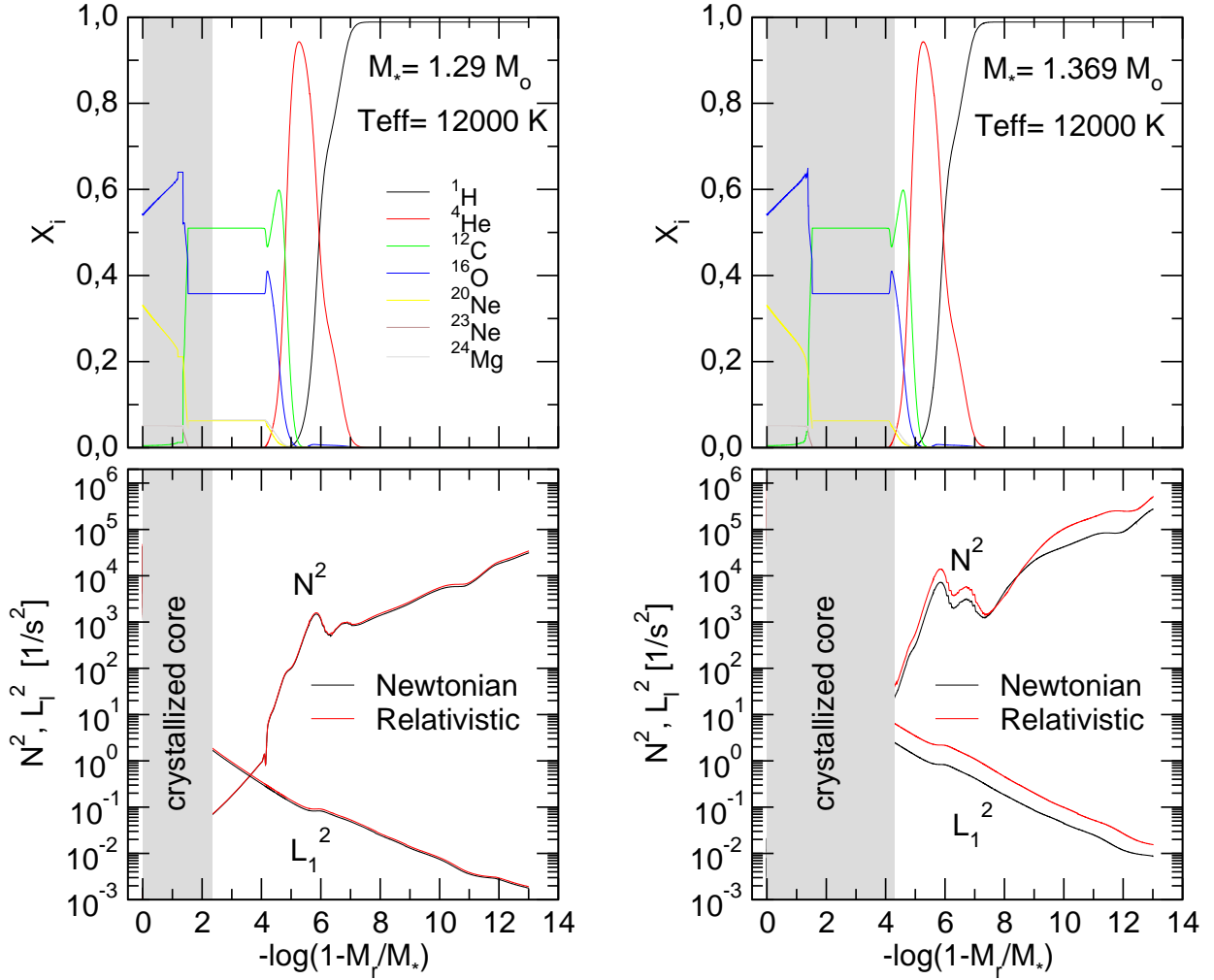


Figure 2: Abundances by mass of the different chemical species as a function of the fractional mass (upper panels), and the logarithm of the squared Brunt-Väisälä and Lamb ($\ell = 1$) frequencies, corresponding to ONe-core DA WD models with $M_* = 1.29 M_\odot$ (left) and $M_* = 1.369 M_\odot$ (right), for $T_{\text{eff}} \sim 12\,000$ K. The gray areas correspond to the crystallized regions.

els for the Newtonian case (black curves) and the relativistic case (red red curves). The triple chemical transition between ^{12}C , ^{16}O , and ^{20}Ne located at $-\log(1 - M_r/M_*) \sim 1.5$ is within the solid part of the core, so it has no relevance for the mode-trapping properties of the models. This is because, according to the “hard-sphere” boundary conditions adopted for the pulsations (Montgomery & Winget, 1999), the g -mode eigenfunctions do not penetrate the crystallized region (gray areas). In this way, the mode trapping properties are entirely determined by the presence of the $^4\text{He}/^1\text{H}$ transition, which is located in more external regions. Note that the Brunt-Väisälä and Lamb frequencies for the Newtonian and relativistic models are indistinguishable for the case of $1.29 M_\odot$, but they notoriously differ when $M_* = 1.369 M_\odot$.

4 Pulsation spectrum of g modes for Newtonian and relativistic ultra-massive WD models

Adiabatic nonradial g -mode Newtonian pulsations have been computed with the LP-PUL pulsation code (Córscico & Althaus, 2006). This code neglects the oscillations of g modes in the crystallized region of the WD core (hard-sphere boundary condition; see Montgomery & Winget, 1999; Córscico et al., 2004). Fig. 3 shows the asymptotic period spacing (computed as in Tassoul et al., 1990) for the sequences of $1.29, 1.31, 1.33, 1.35$ and $1.369 M_\odot$ WD models in terms of the effective temperature all along the ZZ Ceti instability strip. We note that the asymptotic period spacing is smaller for the case of the relativistic WD sequences as compared with the Newtonian sequences. This is what we expect since the asymptotic period

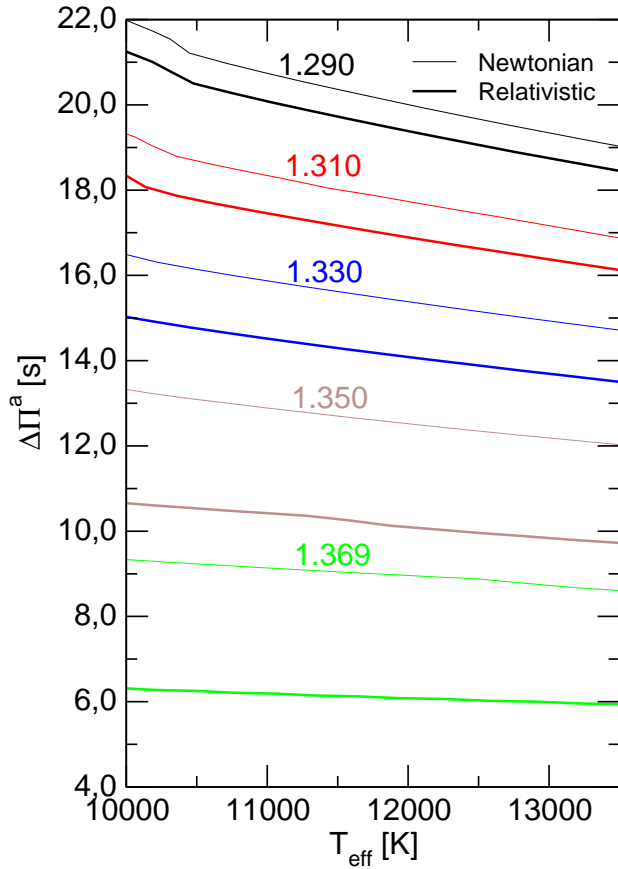


Figure 3: The $\ell = 1$ asymptotic period spacing for WD sequences with different stellar masses for the Newtonian and relativistic cases in terms of T_{eff} through the whole ZZ Ceti instability strip.

spacing is inversely proportional to the integral of the Brunt-Väisälä frequency divided by the radius. Since the Brunt-Väisälä frequency is larger for the relativistic case (see Fig. 2), then the integral is larger and its inverse smaller than in the Newtonian case. The difference is larger for larger stellar masses.

In Fig. 4 we depict the dipole $\ell = 1$ forward period spacing, the kinetic oscillation energy, and the rate of period change for the models with $1.29M_{\odot}$ and $1.369M_{\odot}$, at $T_{\text{eff}} = 12000$ K. We can see that, in general, the period spacing is larger in the Newtonian case, as expected (see Fig. 3). On the other hand, the oscillation kinetic energy of the modes is higher in the relativistic case, since the WDs are more compact and dense than in the Newtonian case. Finally, the rate of change of periods is larger for the relativistic case, since the cooling timescale is shorter due to relativistic effects, in comparison with the Newtonian case (Althaus et al., 2022).

5 Summary and conclusions

In order to start the study of the impact of General Relativity on the pulsations of ultra-massive WDs representative of ZZ Ceti stars, we have calculated as an initial step the Newtonian g -mode pulsations on relativistic equilibrium WD structures. We have found that the Brunt-Väisälä frequency, the period spacing, the oscillation kinetic energy, and the rates of period change are remarkably modified in relation to Newtonian models for the case of very high masses, close to the Chandrasekhar mass, although the effects are much less noticeable for lower masses. The next step in this project is to compute the additional effects of General Relativity on the stellar pulsations by solving the nonradial stellar pulsation equations in the relativistic Cowling approximation. This will allow us to assess the combined effect of General Relativity on the equilibrium structures and on the pulsation modes.

Acknowledgments

A.H.C. warmly thanks Klaus Werner and the Local Organizing Committee of the 22th European White Dwarf Workshop for support that allowed him to attend this conference.

References

- Althaus L. G., Córscico A. H., Isern J., García-Berro E., 2010, *A&A Rev.*, 18, 471
- Althaus L. G., et al., 2020, *A&A*, 633, A20
- Althaus L. G., Camisassa M. E., Torres S., Battich T., Córscico A. H., Rebassa-Mansergas A., Raddi R., 2022, *A&A*, 668, A58
- Camisassa M. E., et al., 2019, *A&A*, 625, A87
- Córscico A. H., Althaus L. G., 2006, *A&A*, 454, 863
- Córscico A. H., García-Berro E., Althaus L. G., Isern J., 2004, *A&A*, 427, 923
- Córscico A. H., Althaus L. G., Miller Bertolami M. M., Kepler S. O., 2019, *A&A Rev.*, 27, 7
- Curd B., Gianninas A., Bell K. J., Kilic M., Romero A. D., Allende Prieto C., Winget D. E., Winget K. I., 2017, *MNRAS*, 468, 239
- Fontaine G., Brassard P., 2008, *PASP*, 120, 1043
- Hermes J. J., Kepler S. O., Castanheira B. G., Gianninas A., Winget D. E., Montgomery M. H., Brown W. R., Harrold S. T., 2013, *ApJ*, 771, L2
- Kanaan A., Kepler S. O., Giovannini O., Diaz M., 1992, *ApJ*, 390, L89
- Montgomery M. H., Winget D. E., 1999, *ApJ*, 526, 976
- Rauer H., et al., 2014, *Experimental Astronomy*, 38, 249

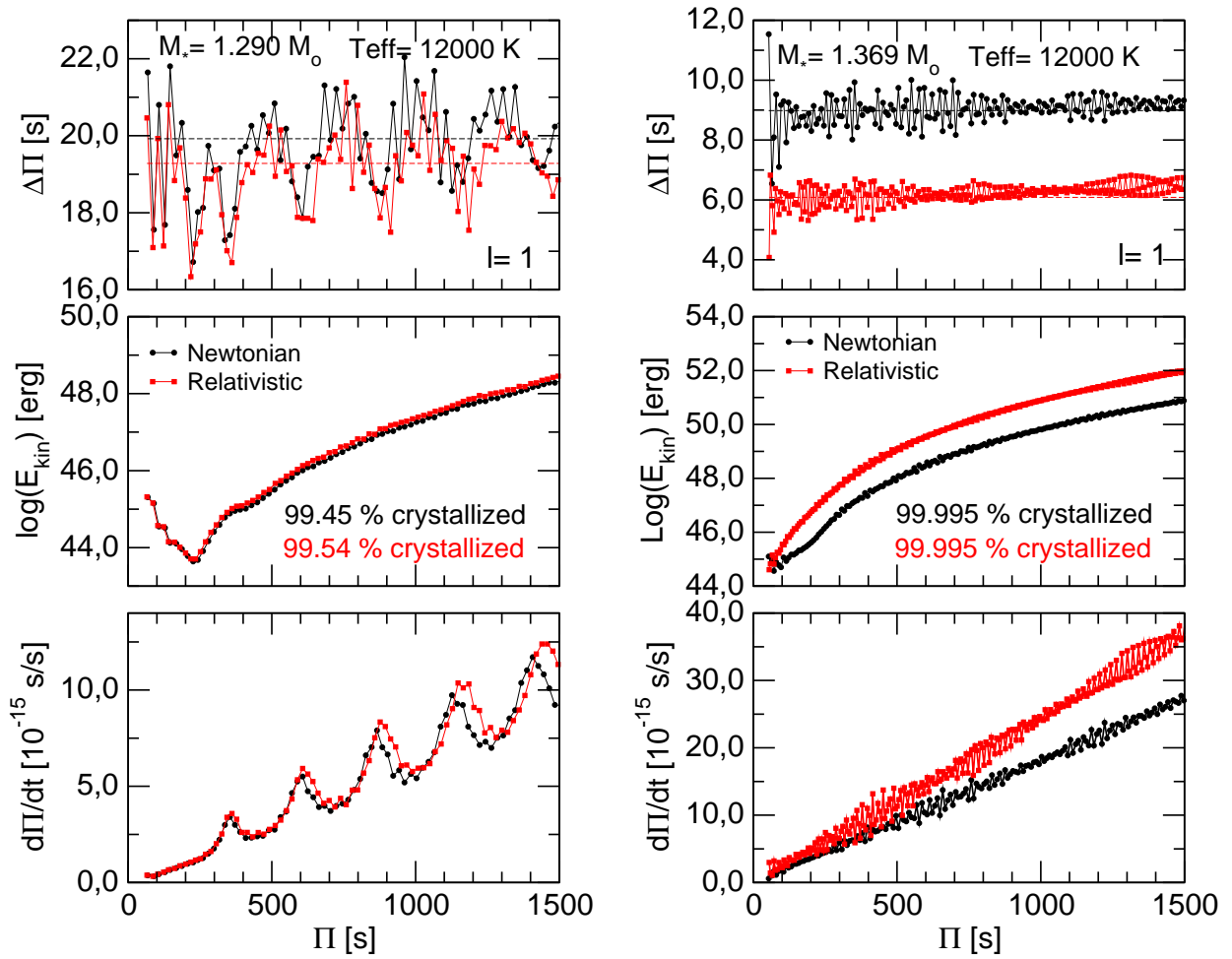


Figure 4: The $\ell = 1$ forward period spacing ($\Delta\Pi = \Pi_{k+1} - \Pi_k$, upper panels), the kinetic energy of oscillation (middle panels), and the rate of period change (lower panels) for models with $1.29M_{\odot}$ (left) and $1.369M_{\odot}$ (right) in the relativistic (red) and Newtonian (black) cases ($T_{\text{eff}} \sim 12000$ K).

Ricker G. R., et al., 2014, in Oschmann Jacobus M. J., Clampin M., Fazio G. G., MacEwen H. A., eds, Society of Photo-Optical Instrumentation Engineers (SPIE) Conference Series Vol. 9143, Space Telescopes and Instrumentation 2014: Optical, Infrared, and Millimeter Wave. p. 914320 (arXiv:1406.0151), doi:10.1117/12.2063489

Rowan D. M., Tucker M. A., Shappee B. J., Hermes J. J., 2019, MNRAS, 486, 4574

Siess L., 2007, A&A, 476, 893

Siess L., 2010, A&A, 512, A10

Tassoul M., Fontaine G., Winget D. E., 1990, ApJS, 72, 335

Thorne K. S., 1977, ApJ, 212, 825

Winget D. E., Kepler S. O., 2008, ARA&A, 46, 157